

# A Reduced High-Order Compact Finite Difference Scheme Based on POD Technique for the Two Dimensional Extended Fisher-Kolmogorov Equation

Baozou Xu, Xiaohua Zhang\*, and Daobin Ji

**Abstract**—In this paper, we mainly utilize the reduced six-order compact finite difference scheme (R-CFDS6) based on proper orthogonal decomposition (POD) and operator splitting method (R-CFDS6-OSM) to solve the two-dimensional Fisher-Kolmogorov equation and extended Fisher-Kolmogorov equation. Toward this end, the CFDS6 is built to attain high accuracy for one-dimensional extended Fisher-Kolmogorov equation. Then by means of the operator splitting method, the two-dimensional extended Fisher-Kolmogorov equation has been converted into a succession of one-dimensional equations successfully, which can be solved easily with CFDS6 compared with Alternating direction implicit method. Finally, by POD method, we develop the R-CFDS6-OSM with fewer unknowns and sufficiently high accuracy to improve the computational efficiency of CFDS6 and furnish the algorithm procedure of R-CFDS6-OSM. Some numerical examples are carried out to validate the high accuracy, effectiveness and feasibility of the R-CFDS6-OSM for the numerical solution of 2D Fisher-Kolmogorov equation.

**Index Terms**—High order compact finite difference scheme, Proper orthogonal decomposition, Operator-splitting method, Extended-Fisher-Kolmogorov equation

## I. INTRODUCTION

THE Fisher-Kolmogorov (FK) equation is considered as a kind of nonlinear partial differential equations named by Fisher and Kolmogorov, which is used to describe the diffusion of organisms and the interaction in adaption. By adding the fourth order derivative term in FK equation, the new model, presented by Coulet [1] and Dee, is called as the extended Fisher-Kolmogorov (EFK) equation. The EFK equation is of important physical background. For example, it is widely applied in sorts of physical phenomena such as the hydrodynamics, plasma physics, thermonuclear reaction, population growth and spread of infectious diseases and so on [2]. However, due to their nonlinearity or the complexity of computing domains, especially when their source term have

no fixed rules, even if there exists the analytical solution [3] theoretically, it isn't easy to find the exact solution for the problem in the actual engineering applications. Thus, finding the numerical solutions becomes a feasible method.

Tracing back to the existing literatures, many numerical solutions including the finite difference scheme (FDM) [4], [5], finite element Galerkin method [6] and collocation method [7], [8] have been published in order to pursue the efficient and accurate numerical methods for the EFK equation or the equation which has similar characters in one and higher dimension. In these methods mentioned above, the FDM is always regarded as the convenient and efficient way for finding the numerical solution of EFK equation because of the easy programming, straightforward and intuitive mathematical expression and wide application in applied fields of sciences. Although some classical numerical schemes such as the central difference or Euler method can be carried out to solve the equation successfully, they converge very slowly and may largely deviate from the exact solution after some computing steps. Therefore, it is imperative for the FK equation to develop a scheme that can guarantee a satisfying numerical solution and reflect the properties of equations.

In the last decades, many scholars focus their eyes on the compact finite difference scheme (CFDS). It has been proved by many researches that the CFDS can lead to higher order accurate approximations with smaller stencils compared with corresponding explicit schemes in each coordinate direction [9], [10], [11]. As one of the most effective numerical implementations, a variety of high-order CFDS have been developed. For instance, Li employed six-order CFDS in space to solve the 2D parabolic equation [12], nonlinear dispersive waves [13]. Feng constructed the compact finite difference for a class of space-time fractional differential equations with the order of the spatial fractional derivative more than two[14]. Deng and Xie proposed two high-order numerical method for the one-dimensional Burgers' equations[15]. The authors in [16] proposed a compact finite-difference method which uses a weighted compact scheme in space and Runge-Kutta methods in time for the accurate simulation of the atmospheric flows Sun constructed an unconditionally stable scheme with combination of CFDS in spatial discretization and Crank-Nicolson scheme for the temporal discretization [17]. Zhai and Feng have introduced a novel method which obtain six-order CFDS based on three different types of dual partitions [18]. Especially, Mohebbi and Dehghan developed High-order compact solution for heat and advection-diffusion [19]. Moreover, they employed high order difference scheme

Manuscript received March 22, 2020; revised June 7, 2020. This work is financially supported by the Engineering Research Center of Eco-environment in Three Gorges Reservoir Region (No. KF-2019-10), and the National Natural Science Foundation of China (Grant No. 11972216).

Baozou Xu is with the Engineering Research Center of Eco-environment in Three Gorges Reservoir Region, Ministry of Education, and the College of Science, China Three Gorges University, Yichang, 443002, China, e-mail:(xubaouzou@163.com).

\*Xiaohua Zhang is corresponding author with the Engineering Research Center of Eco-environment in Three Gorges Reservoir Region, Ministry of Education, and the College of Science, China Three Gorges University, Yichang, 443002, China, e-mail:(zhangxiaohua07@163.com).

Daobin Ji is with the Engineering Research Center of Eco-environment in Three Gorges Reservoir Region, Ministry of Education, China Three Gorges University, Yichang, 443002, China, e-mail:(394816707@qq.com).

and radial basis functions meshless approach for the fractional Rayleigh-Stokes problem [20]. However, the CFDS6 for EFK and FK equations, especially the case of desirable accuracy in high dimension, they usually need small spatial discretization or extended finite difference stencils and a small time step which brings heavily computational loads. Therefore, an important problem for CFDS6 is how to build a scheme which not only saves the computational time in the practical problems but also holds a sufficiently accurate numerical solution.

A large number of numerical examples have proved that the proper orthogonal decomposition (POD) is an effective and feasible technique, which can provide the adequate approximation for numerical models with fewer unknowns. It can vastly alleviate the computational loads under guaranteeing the sufficiently accurate solution. The POD is also known as Karhunen-Loève expansions in signal analysis or principal component analysis in statistics, which has been extensively used in the real-life application. Especially, it has been applied to some reduced models including finite element methods and finite volume element method [21], [22], meshless method [23], finite difference method [24] successfully. Nevertheless, most of these methods based on POD are restricted to problems involving first and second spatial derivatives. There are no papers concerning with reduced high-order compact finite difference scheme based on POD has been carried out for EFK equation involving fourth derivatives and mixed derivatives. Thus, the first task in this paper is to build the R-CFDS6 based on POD for solving the EFK and FK equations

Alternating Direction Implicit(ADI) method is a classical scheme to manage the multi-dimensional problem. The main idea of ADI method is that the sets of one-dimensional problems can be obtained by different method in the discretization of space and time. Since each one-dimensional problem in each time step usually requires tridiagonal matrices to solve, this way is feasible to deal with multi-dimensional problem. Nevertheless, the accuracy of ADI only has second order, which generates the accumulation of the truncated errors in the process of computation. Especially, ADI may produce considerable dissipation because it is complex to implement in the program of computer and it requires a large amount of computational effort. Thus, a crucial issue for multi-dimensional problem is how to build more accurate or convenient scheme. The authors of [25] solve the Burgers' equation by introducing the splitting technique that splits it into two sub-equations. Then each sub-equation can be solved by different FDM. Similar with that, coupled with cubic spline method, there are two-time-level splitting [26] and three-time-level splitting technique [27] for solving the Burgers' equation. In [28], the authors have split the full problem into hyperbolic, nonlinear and linear problem, then different numerical method can be used for the numerical solution of each of them. Sun [29] gave the framework of splitting method for the radiative transfer problem. Therefore, Operator splitting method (OSM) is an efficient method to solve multi-dimensional problem and nonlinear equation. To the best knowledge of authors, no high-order CFDS combined with POD and OSM (R-CFDS6-OSM) aimed to solve two-dimensional EFK and FK equations efficiently has been developed so far. Hence, the second task in this paper is to

develop the R-CFDS6-OSM based on POD and OSM method to attain high accurate numerical solution of two-dimensional EFK and FK equations, which only contains very fewer unknowns and simplifies whole process of computation.

The rest of this paper is arranged as follows. In Section II, we build the CFDS6 for the one-dimensional EFK equations and give the stability analysis. In Section III, the splitting method is illustrated and the whole detailed procedure of the algorithm is given. In Section IV, the R-CFDS6-OSM based on the POD technique for the 2D EFK equation is established. In Section V, we utilize four numerical examples to demonstrate the reliability and effective of this algorithm. Section VI provides the main conclusions and discussion.

## II. THE CONSTRUCTION OF HIGH-ORDER COMPACT FINITE DIFFERENCE SCHEME

We consider the following 1D EFK equation.

$$\begin{cases} u_t + \gamma \frac{\partial^4 u}{\partial x^4} - \frac{\partial^2 u}{\partial x^2} + f(u) = g, & a \leq x \leq b, 0 < t \leq T, \\ u(x, 0) = u_0, & a \leq x \leq b, \\ u(a, t) = u(b, t) = 0, & a \leq x \leq b, 0 < t \leq T, \\ u_{xx}(a, t) = u_{xx}(b, t) = 0, & a \leq x \leq b, 0 < t \leq T. \end{cases} \quad (1)$$

The form of  $f(u)$  occurs most in applications is that  $f(u) = u^3 - u$  and  $\gamma$  is a constant. We first divide the time span  $[0, T]$  into  $K$  time steps, which means that the time increment  $\tau = T/K$  and  $T = k \cdot \tau$ ,  $k = 1, 2, \dots, K$ . The uniform 1D mesh is consist of  $N$  points. The spatial step is  $h = (b - a)/N$ .  $x_i = (i - 1) \cdot h$ ,  $i = 1, 2, \dots, N$ .

According to different discretization in space, the CFDS can be classified into two broad categories. The first step of first ones is to apply central difference to the governing partial differential equation. Then, the higher-order derivatives in the truncation error are constantly replaced with low-order derivatives of the partial differential equation, which is called the traditional explicit finite differences. Based on the Taylor expansion, the main idea of second ones is that the spatial derivatives of  $u$  can be approximated by solving a system of linear equations for any scalar value  $u$ . In this paper, we choose the second way to build high-order compact finite difference scheme for EFK equation.

The technique in [10] has implied that the derivatives of  $u$  can be obtained by solving a diagonal system. For more details on the whole derivation, please refer to [10], [30], which will not be described here again. In the following, we just list the final formulae of an implicit sixth-order compact finite difference scheme.

For the approximate second-order derivatives at interior nodes, the sixth-order scheme is given by the following:

$$\frac{2}{11} u''_{i-1} + u''_i + \frac{2}{11} u''_{i+1} = \frac{3}{44h^2} (u_{i+2} - u_i + u_{i-2}) + \frac{12}{11h^2} (u_{i+1} - 2u_i + u_{i-1}). \quad (2)$$

For the approximate fourth-order derivatives at interior nodes, the sixth-order scheme is given by the following:

$$\begin{aligned} \frac{7}{26} u''''_{i-1} + u''''_i + \frac{7}{26} u''''_{i+1} &= \frac{1}{h^4} \left( \frac{1}{78} u_{i-3} + \frac{19}{13} u_{i-2} \right. \\ &\quad \left. - \frac{465}{78} u_{i-1} + \frac{700}{78} u_i - \frac{465}{78} u_{i+1} + \frac{19}{13} u_{i+2} + \frac{1}{78} u_{i+3} \right). \end{aligned} \quad (3)$$



III. THE ESTABLISHMENT OF CFDS6 FOR THE 2D EFK EQUATION

The ADI method proposed by Peaceman and Rachford [32] is a well-known method to solve multi-dimensional problems, which replaces multi-dimensional problems with a number of one-dimensional problems. Nevertheless, the accuracy of ADI is found that it only has second order accuracy. Besides, this method may result a complicated set of equations, which is very expensive to solve. The benefits of ADI method are that the equation in each step can be solved by the tri-diagonal matrix algorithm successfully. Nevertheless, the ADI method for two-dimensional EFK equation, they usually need more advanced way to deal with the mixed derivatives. Compared with ADI, operator splitting method (OSM) is an effective numerical method for solving multi-dimensional problems by converting it to a series of one-dimensional problems and the programming is very simple. It also can be used to accelerate that calculation of problems relate to operators of different time scales. In this section, instead of using ADI, we use CFDS6-OSM to solve 2D EFK equation. First, we apply OSM to decompose it into sub-equation. Then, we solve each sub-equation by CFDS6.

A. The detailed methods for 2D EFK equation

The authors in [33] have developed high order splitting methods for the numerical solutions of one dimensional Burgers' equation with periodic, Dirichlet, Neumann and Robin boundary conditions. Motivated by the idea, the 2D EFK equation is split as follows:

For the following 2D EFK equation.

$$\begin{cases} u_t + \gamma \Delta^2 u - \Delta u + f(u) = g, & (x, y, t) \in \Omega \times (0, T], \\ u(x, y, 0) = u_0(x, y), & (x, y) \in \Omega, \\ u = 0, \Delta u = 0, & (x, y, t) \in \partial\Omega \times (0, T], \end{cases} \quad (13)$$

where the  $\Delta$  is the Laplace operator and  $f(u) = u^3 - u$ . Let  $\Omega = (0, a_2) \times (0, b_2)$ ,  $N_x$  and  $N_y$  be any positive integers,  $h_x = a_2/(N_x - 1)$ ,  $h_y = b_2/(N_y - 1)$ ,  $x_i = (i - 1)h_x$ ,  $y_j = (j - 1)h_y$ ,  $i = 1, 2, \dots, N_x$ ,  $j = 1, 2, \dots, N_y$ . In this work, for the convenience of computation, we let  $h_x = h_y$  and  $N_x = N_y$ .  $u_{i,j}^n \approx u(x_i, y_j, t_n)$ .

The Eq. (13) has been split into:

$$\frac{d\mathbf{u}_1}{dt} = -f(\mathbf{u}_1) + \mathbf{g} \quad (14)$$

$$\frac{d\mathbf{u}_2}{dt} = \frac{\partial^2 \mathbf{u}_2}{\partial x^2} - \gamma \frac{\partial^4 \mathbf{u}_2}{\partial x^4} \quad (15)$$

$$\frac{d\mathbf{u}_3}{dt} = \frac{\partial^2 \mathbf{u}_3}{\partial y^2} - \gamma \frac{\partial^4 \mathbf{u}_3}{\partial y^4} \quad (16)$$

$$\frac{d\mathbf{u}_4}{dt} = -2\gamma \frac{\partial^4 \mathbf{u}_4}{\partial x^2 \partial y^2} \quad (17)$$

Authors in [34] presented the OSM for particular examples of the PDEs with Burgers' nonlinearity, where the convergence of the Strang splitting method and theory for the equation in Sobolve spaces is given. In [35], they analyze operator splitting for the Benjamin-Ono equation and show the convergence of both Godunov and Strang splitting methods. Especially, in [36], the authors have applied the

iterative operator splitting method on the Korteweg-de Vries (KdV) equation, which is similar with our schemes. Firstly, splitting the complex problem into simpler sub-problems. Secondly, each sub-equation is solved with iterative schemes. In addition, they also have presented the stability criteria of their method applied to the KdV equation with Von Neumann analysis. Therefore, similar convergence and stability analysis can be expected for the Eq. (13)-(17).

B. The CFDS6 for the sub-problem

Each sub-problem in Eq. (13)-(17) can be solved by the CFDS6. In the following, we will give the specific implementation of the CFDS6-OSM for the 2D EFK equations. We denote the  $\mathbf{u}_{\cdot,j} = (u_{1,j}, u_{2,j}, \dots, u_{N_x,j})^T$  and  $\mathbf{u}_i = (u_{i,1}, u_{i,2}, \dots, u_{i,N_y})^T$ .

**Algorithm 1** Implementation of the CFDS6-OSM for the 2D EFK equations

- 1: Compute the initial value of  $u_{i,j}^0$  ( $i = 1, 2, \dots, N_x$ .  $j = 1, 2, \dots, N_y$ )
- 2: **for**  $k = 1, 2, \dots, K$  **do**
  - (a) Compute the Eq. (14) by the Eq. (7)-(8) with  $L_1(\mathbf{u}) = \mathbf{u} - \mathbf{u}^3$  and  $L_2(\mathbf{g}) =$ 
    - i. Compute the  $f_{i,j} = (u_{i,j}^{k-1})^3 - u_{i,j}^{k-1}$  for the domain ( $i = 1, 2, \dots, N_x$ .  $j = 1, 2, \dots, N_y$ ) in Eq. (14).
    - ii. Compute the  $g_{i,j}^{k-1} = g(x_i, y_j, (k - 1) \cdot \tau)$ ,  $g_{i,j}^{k-0.5}$  and  $g_{i,j}^k$  in Eq. (14). The computational domain is same as  $f_{i,j}$ .
    - iii. Do  $j = 1, 2, \dots, N_y$  Computer the  $\mathbf{u}_{1,j}^k$  by the Eq. (8).
  - (b) Compute the Eq. (15) by the Eq. (7)-(8) with  $L_1(\mathbf{u}) = \frac{\partial^2 \mathbf{u}_2}{\partial x^2} - \gamma \frac{\partial^4 \mathbf{u}_2}{\partial x^4}$  and  $L_2(\mathbf{g}) = 0$ .
    - i. Do  $j = 1, 2, \dots, N_y$  Compute the  $(\mathbf{u}_{2xx})_{\cdot,j} = \mathbf{B}_2^{-1} \mathbf{A}_2 \mathbf{u}_{1,j}^k$  and  $(\mathbf{u}_{2xxxx})_{\cdot,j} = \mathbf{B}_4^{-1} \mathbf{A}_4 \mathbf{u}_{1,j}^k$  in Eq. (15).
    - ii. Do  $j = 1, 2, \dots, N_y$  Computer the  $\mathbf{u}_{2,j}^k$  by the Eq. (8).
  - (c) Compute the Eq. (16) by the Eq. (7)-(8) with  $L_1(\mathbf{u}) = \frac{\partial^2 \mathbf{u}_3}{\partial y^2} - \gamma \frac{\partial^4 \mathbf{u}_3}{\partial y^4}$  and  $L_2(\mathbf{g}) = 0$ .
    - i. Do  $i = 1, 2, \dots, N_x$  Compute the  $(\mathbf{u}_{3yy})_{i,\cdot} = \mathbf{B}_2^{-1} \mathbf{A}_2 \mathbf{u}_{2,i}^k$  and  $(\mathbf{u}_{3yyy})_{i,\cdot} = \mathbf{B}_4^{-1} \mathbf{A}_4 \mathbf{u}_{2,i}^k$  in Eq. (16).
    - ii. Do  $i = 1, 2, \dots, N_x$  Computer the  $\mathbf{u}_{3,i}^k$  by the Eq. (8).
  - (d) Compute the Eq. (17) by the Eq. (7)-(8) with  $L_1(\mathbf{u}) = -2\gamma \frac{\partial^4 \mathbf{u}_4}{\partial x^2 \partial y^2}$  and  $L_2(\mathbf{g}) = 0$ .
    - i. Do  $i = 1, 2, \dots, N_x$  Compute the  $(\mathbf{u}_{4yy})_{i,\cdot} = \mathbf{B}_2^{-1} \mathbf{A}_2 \mathbf{u}_{3,i}^k$ .
    - ii. Do  $j = 1, 2, \dots, N_y$  Compute the  $(\mathbf{u}_{4yyxx})_{\cdot,j} = \mathbf{B}_2^{-1} \mathbf{A}_2 (\mathbf{u}_{4yy})_{\cdot,j}^k$ .
    - iii. Do  $j = 1, 2, \dots, N_y$  Computer the  $\mathbf{u}_{\cdot,j}^k$  by the Eq. (8).

IV. ESTABLISHMENT OF THE R-CFDS6-OSM FOR THE 2D FISHER-KOLMOGOROV EQUATION

We have listed the details of implementation of CFDS6-OSM for the high accuracy numerical solution of EFK

equation. Although the CFDS6-OSM for the EFK equation has been posed above, it usually either needs small spatial discretization or extended finite difference stencils and a small time step which results in computational expensive calculations. Therefore, a key issue in practical engineering problems is that how to build a reduced-order scheme possesses the fewer unknowns so as to ease the computational burden and gains the sufficiently high accuracy of the CFDS6-OSM. As described in the Introduction, the POD is an effective way to reduce the unknowns of original scheme while guaranteeing the the sufficiently accurate numerical solutions for the original scheme. Hence, in the following, we first illustrate the details about the formulation of POD basis, then the R-CFDS6-OSM is established for the EFK equation.

A. The procedure of formulating the POD basis

The whole procedures can be summarized as follows:

**Step 1.** The construction of snapshots

Let  $u_m^k = u_{i,j}^k, (1 \leq m = (j - 1) \cdot N_x + i \leq M = N_x \cdot N_y, 1 \leq i \leq N_x, 1 \leq j \leq N_y, 0 \leq k \leq K)$ . Then, the CFDS6-OSM solutions can be denoted by the set  $\{u_m^k\}_{k=1}^K (1 \leq m \leq M)$ . Firstly, we gain the first  $L (L \leq K)$  sequence of the CFDS6-OSM solutions  $\{u_m^k\}_{k=1}^L (1 \leq m \leq M, L \leq K)$  for the Eq. (15) as snapshots, then we get the snapshots which can be expressed as the  $M \times L$  snapshot matrices.

$$D = \begin{pmatrix} u_1^1 & u_1^2 & \cdots & u_1^k & \cdots & u_1^L \\ u_2^1 & u_2^2 & \cdots & u_2^k & \cdots & u_2^L \\ \vdots & \vdots & \ddots & & & \vdots \\ u_m^1 & u_m^2 & \cdots & u_m^k & \cdots & u_m^L \\ \vdots & \vdots & & & \ddots & \vdots \\ u_M^1 & u_M^2 & \cdots & u_M^k & \cdots & u_M^L \end{pmatrix}$$

Although the snapshot in this paper is obtained through the CFDS6-OSM solution, in fact, the collection of snapshots can be constructed through experiments and interpolation when calculating the actual problem. For example, for some natural phenomena such as weather change and biology anagenesis, if the development and change are closely related to previous results, or if the physical system of the natural phenomena performs well, that is, the past dynamics is representative and inclusive of the future dynamics, then the previous or existing data from experiment can be used to formed a snapshot. Then the POD basis is obtained via using the POD method mentioned as follows and we can derive an efficient scheme with fewer unknowns. Therefore, the development and change of some future natural phenomena can be effectively calculated and predicted, which has important applied prospect for realistic applications.

**Step 2.** The singular value decomposition for the snapshot  $D$

By the singular value decomposition, we have

$$D = U \begin{pmatrix} S_{r \times r} & O_{r \times (L-r)} \\ O_{(M-r) \times r} & O_{(M-r) \times (L-r)} \end{pmatrix} V^T$$

where  $S_{r \times r} = \text{diag}\{\sigma_1, \sigma_2, \dots, \sigma_r\}$ . The  $\sigma_i (i = 1, 2, \dots, r)$  is the singular value of  $D$ , which satisfy the relations of  $\sigma_1 \geq \sigma_2 \geq \dots \geq \sigma_r > 0. r = \text{rank}(D)$ .

$U = (\alpha_1, \alpha_2, \dots, \alpha_M)$  is an  $M \times M$  orthogonal matrix,  $\alpha_i (i = 1, 2, \dots, M)$  are the eigenvectors of  $DD^T$  arranged corresponding to the order of  $\sigma_i (i = 1, 2, \dots, r)$ .  $V_{L \times L} = (\chi_1, \chi_2, \dots, \chi_L)$  is orthogonal matrix and  $\chi_i (i = 1, 2, \dots, L)$  is the eigenvectors of  $D^T D$ . It should be noted that the arrangement of  $\chi_i$  is the same as  $\alpha_i$ .

It is clearly to find that the number of mesh points  $M$  is much larger than the that of snapshots  $L$  extracted from the CFDS6-OSM solutions. Since there exists the  $M \gg L$ , it can be concluded that the degree of  $DD^T$  is much larger than the degree of  $D^T D$ . Especially, the positive eigenvalues  $\lambda_i = \sigma_i^2$  of  $D^T D$  and  $DD^T$  are identical.

Hence, we can first obtain the eigenvalues  $\lambda_i$  for the matrix  $D^T D$  and the associated eigenvectors  $\chi_i$ . By using the following formulae:

$$\alpha_i = \frac{1}{\sigma_i} D \chi_i, \quad i = 1, 2, \dots, r$$

we can compute the eigenvectors  $\alpha_i (1 \leq i \leq r \leq L)$  corresponding to the nonzero eigenvalues for matrix  $D^T D$ .

Choose

$$D_d = U \begin{pmatrix} S_{d \times d} & O_{d \times (L-d)} \\ O_{(M-d) \times d} & O_{(M-d) \times (L-d)} \end{pmatrix} V^T,$$

where  $S_{d \times d} = \text{diag}\{\sigma_1, \sigma_2, \dots, \sigma_d\}$ . Thus we have the following formulae

$$D_d = \alpha \alpha^T D, \quad \alpha = (\alpha_1, \alpha_2, \dots, \alpha_d).$$

**Step 3.** The construction of POD basis

The  $\|D\|_{2,2} = \sup_{u \in R^L} \frac{\|Du\|_2}{\|u\|_2}$  is the norm of matrices  $D$ , where the  $\|u\|_2$  is the norm for vector  $u$ . By the relationship between the matrix norm and its spectral radius [37], we have the following:

$$\|D - D_d\|_{2,2} = \|D - \alpha \alpha^T D\|_{2,2} = \sqrt{\lambda_{d+1}} \quad (18)$$

The  $L$  column vectors of  $D$  is denoted as  $u^k = (u_1^k, u_2^k, \dots, u_m^k, \dots, u_M^k)^T (k = 1, 2, \dots, L)$ , we have the following:

$$\|u^k - u_d^k\|_2 = \|(D - D_d)\varepsilon_k\|_2 \leq \|D - D_d\|_{2,2} \|\varepsilon_k\|_2 = \sqrt{\lambda_{d+1}} \quad (19)$$

The  $\varepsilon_k$  represents the unit vector with  $n$ th component being 1.  $u_d^k = D_d \varepsilon_k = \alpha \alpha^T D \varepsilon_k = \sum_{j=1}^d (\alpha_j, u^k) \alpha_j$ , where the  $(\alpha_j, u^k)$  denotes the inner product of  $\alpha_j$  and  $u^k$ . In a word, the  $u_d^k$  is the projection of the  $u^k$  onto the subspace span  $\{\alpha_1, \alpha_2, \dots, \alpha_d\}$ . The inequality Eq. (19) has illustrated that the  $u_d^k$  is the optimal approximation of  $u^k$  under the error between them is no more than  $\sqrt{\lambda_{d+1}}$ . Therefore,  $\alpha$  is an orthogonal optimal POD basis of  $D$ .

B. Establishment of the R-CFDS6-OSM

In this sub-section, we will utilize the POD basis to construct the reduced model for the Eq. (15). In Eq. (15), the  $u^k = (u_1^k, u_2^k, \dots, u_m^k, \dots, u_M^k)^T (1 \leq k \leq K)$ . By the POD basis  $\alpha$ , we get the R-CFDS6-OSM solution  $u_d^k = \alpha \alpha^T D \varepsilon_k = \alpha \alpha^T u^k$  and we put it in Eq. (8) to replace  $u^k$  by

$$u_d^k = \alpha V_d^k \quad (20)$$

where the  $\mathbf{V}_d^k = (v_1^k, v_2^k, \dots, v_d^k)^T$ . For the  $\mathbf{u}^k$ , we can use the following formulae to obtain their second-order derivatives and fourth-order derivatives:

$$\mathbf{u}'' = \mathbf{C}_1 \mathbf{u} \tag{21}$$

$$\mathbf{u}'''' = \mathbf{C}_2 \mathbf{u} \tag{22}$$

where

$$\mathbf{C}_1 = \begin{pmatrix} \mathbf{B}_2^{-1} \mathbf{A}_2 & 0 & \dots & 0 \\ 0 & \mathbf{B}_2^{-1} \mathbf{A}_2 & \ddots & \vdots \\ \vdots & \ddots & \ddots & 0 \\ 0 & \dots & \dots & \mathbf{B}_2^{-1} \mathbf{A}_2 \end{pmatrix}_{M \times M}$$

$$\mathbf{C}_2 = \begin{pmatrix} \mathbf{B}_4^{-1} \mathbf{A}_4 & 0 & \dots & 0 \\ 0 & \mathbf{B}_2^{-1} \mathbf{A}_2 & \ddots & \vdots \\ \vdots & \ddots & \ddots & 0 \\ 0 & \dots & \dots & \mathbf{B}_4^{-1} \mathbf{A}_4 \end{pmatrix}_{M \times M}$$

By multiplying the  $\alpha^T$  in the left hand of Eq. (4) and Eq. (5), we can get the reduced second-order derivatives and fourth-order derivatives:

$$(\alpha^T)_{d \times M} (\mathbf{u}^{k''})_{M \times 1} = (\alpha^T \mathbf{C}_1 \alpha)_{d \times d} (\mathbf{V}_d^k)_{d \times 1} \tag{23}$$

$$(\alpha^T)_{d \times M} (\mathbf{u}^{k''''})_{M \times 1} = (\alpha^T \mathbf{C}_2 \alpha)_{d \times d} (\mathbf{V}_d^k)_{d \times 1} \tag{24}$$

Similar with the way mentioned in Eq. (7), the Eq. (15) also can be written in the form of ODE

$$\frac{d\mathbf{u}}{dt} = L_1(\mathbf{u}) \tag{25}$$

In the Eq. (8), the CFDS6 is given. Let  $\mathbf{V}_0 = \alpha^T \mathbf{u}^k$ , we can achieve the R-CFDS6 for Eq. (15) as follows:

$$\begin{cases} \bar{\mathbf{k}}_0 = \tau \cdot L_1(\mathbf{V}_0), & \mathbf{V}_1 = \mathbf{V}_0 + \bar{\mathbf{k}}_0/2, \\ \bar{\mathbf{k}}_1 = \tau \cdot L_1(\mathbf{V}_1), & \mathbf{V}_2 = \mathbf{V}_0 + \bar{\mathbf{k}}_1/2, \\ \bar{\mathbf{k}}_2 = \tau \cdot L_1(\mathbf{V}_2), & \mathbf{V}_3 = \mathbf{V}_0 + \bar{\mathbf{k}}_2, \\ \bar{\mathbf{k}}_3 = \tau \cdot L_1(\mathbf{V}_3), & \bar{\mathbf{K}} = \bar{\mathbf{k}}_0 + 2\bar{\mathbf{k}}_1 + \bar{\mathbf{k}}_2 + \bar{\mathbf{k}}_3, \\ \mathbf{V}^{k+1} = \mathbf{V}_0 + \frac{1}{6} \bar{\mathbf{K}}, & \mathbf{u}_d^{k+1} = \alpha \mathbf{V}^{k+1}. \end{cases} \tag{26}$$

We have achieved the R-CFDS6-OSM solution vector  $\mathbf{u}_d^{k+1}$  by solving the Eq. (23)-(26) which only involves  $d(d \ll M)$  unknowns. Hence, in the similar way, we also can achieve the R-CFDS6-OSM solution for Eq. (16). It can be easily understood that the CFDS6-OSM on each time step includes  $M$  unknowns while the R-CFDS6-OSM on each time step only contains  $d(d < L \ll M)$  unknowns. Therefore, it has been confirmed that the R-CFDS6-OSM can save the CPU time required for computation, which is far superior to the CFDS6-OSM for the 2D Fisher-Kolmogorov equation.

### V. NUMERICAL EXAMPLES

In order to see whether the present method is capable of getting an accurate solution, in this section, the CFDS6-OSM will be evaluated for four EFK or FK examples given below. In the case of the different number of nodes, we have some tests of accuracy and efficiency for the method described in this article. We performed our computations using Matlab 2018a software on a Ryzen 7 1800X, 3.6 GHz CPU machine with 16 GB of memory. The convergence order of the method

presented in this article is calculated with this formula

$$R = \frac{\log \frac{error_{new}}{error_{old}}}{\log \frac{h_{new}}{h_{old}}}$$

**Example 1:** We consider the following 1D EFK equation(SP<sub>1</sub>)

$$\begin{cases} \frac{\partial u}{\partial t} + \gamma \frac{\partial^4 u}{\partial x^4} - \frac{\partial^2 u}{\partial x^2} + f(u) = g(x, t), & (x, t) \in \Omega \times (0, 1] \\ u(x, 0) = \sin(x), & 0 \leq x \leq 2\pi, \\ u(0, t) = u(1, t) = 0, & 0 < t \leq 1. \end{cases}$$

Exact solution of problem is given by  $u(x, t) = e^{-t} \sin(x)$  for  $x \in \Omega = [0, 2\pi]$  and  $t \in [0, 1]$ .  $\gamma = 2$  and  $g(x, t) = e^{-3t} \sin(x)^3 + e^{-t} \sin(x)$ .

The derivatives of SP<sub>1</sub> is approximated by the Eq. (2)-(5) and  $\gamma = 2$ . To verify the convergence of CFDS6, we fix time increment  $\tau = 0.000001$  and decrease the spatial step from 1/10 to 1/80 in Table I. Table I also presents the maximum error of CFDS6 and computational time for different distributed points. It shows that CFDS6 has achieved the expected sixth order accuracy, which is confirmed by solving the SP<sub>1</sub> with various mesh sizes. Figure 1-2 depicts the numerical solution and error of CFDS6 Eq. (8) with  $h = 0.025\pi$  at  $T = 1$ . It is obviously noted that these computed results are in good agreement with the exact solution of SP<sub>1</sub>.

TABLE I  
THE CONVERGENCE ORDER AND MAXIMUM ERROR FOR SP<sub>1</sub> AT  $t = 1$

	Nodes	21 × 21	41 × 41	81 × 81
CFDS6-OSM	Max(error)	1.6814e-07	2.6119e-09	5.1793e-11
	Time(s)	31.325176	56.985801	116.380887
	Order	-	6.0084	5.6562

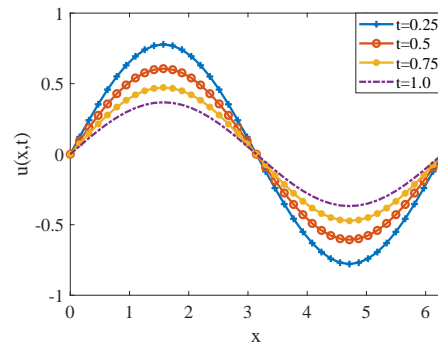


Fig. 1. The CFDS6(N = 41) solution at  $t = 0.25, 0.5, 0.75, 1.0$  for SP<sub>1</sub>.

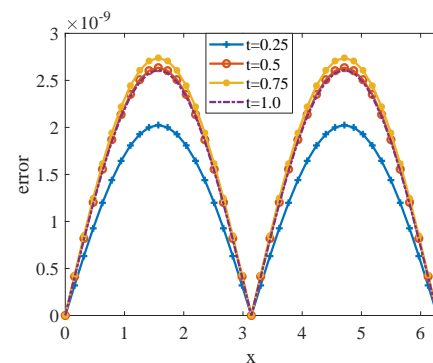


Fig. 2. The CFDS6(N = 41) error at  $t = 0.25, 0.5, 0.75, 1.0$  for SP<sub>1</sub>.

**Example 2:** We consider the following 1D EFK equation(SP<sub>2</sub>)

$$\begin{cases} \frac{\partial u}{\partial t} + \gamma \frac{\partial^4 u}{\partial x^4} - \frac{\partial^2 u}{\partial x^2} + f(u) = 0, & 0 \leq x \leq 2\pi, 0 < t \leq 1 \\ u(x, 0) = \sin(x), & 0 \leq x \leq 2\pi, \\ u(0, t) = u(1, t) = 0, & 0 < t \leq 1. \end{cases}$$

The exact solution of SP<sub>2</sub> is absent. We let  $\gamma = 2$ . We take the numerical solution when  $N = 81$  in CFDS6 as the exact solution  $u$  approximately so as to get the maximum absolute error in different nodes and verify the convergence of our scheme. This problem contains a fourth-order derivative, which also can be approximated by the Eq. (2)-(5). we fix time increment  $\tau = 0.000001$  in the computation. when  $h$  is reduced by a factor of 2, the maximum error of  $u$  is reduced by a factor of  $2^6$ , which is confirmed by the data in the Table II. In addition, Table II presents the maximum error of CFDS6 and computational time for different distributed points. The maximum absolute error is  $6.3842 \times 10^{-6}$  when  $N = 11$ , which shows that CFDS6 can still successfully produce very accurate solution via significantly coarse grid. Figure 3-4 plots the numerical solution of SP<sub>2</sub> with  $N = 41$ , which indicates that the spatial error is rapidly smaller and almost negligible.

TABLE II  
THE CONVERGENCE ORDER AND MAXIMUM ERROR FOR SP<sub>2</sub> AT  $t = 1$

	Nodes	11 × 11	21 × 21	41 × 41
CFDS6-OSM	Max(error)	6.3482e-06	1.0096e-07	1.5374e-09
	Time(s)	0.992494	1.591310	2.906707
	Order	-	5.9745	6.0371

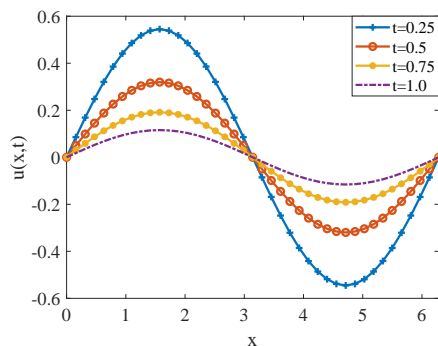


Fig. 3. The CFDS6( $N = 41$ ) solution at  $t = 0.25, 0.5, 0.75, 1.0$  for SP<sub>2</sub>.

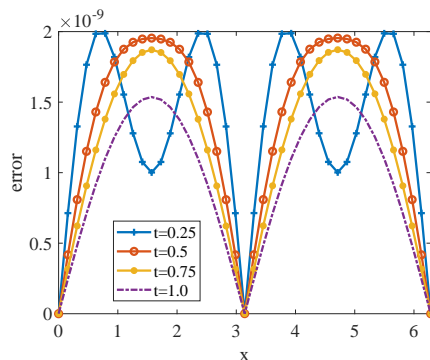


Fig. 4. The CFDS6( $N = 41$ ) error at  $t = 0.25, 0.5, 0.75, 1.0$  for SP<sub>2</sub>.

**Example 3:** We consider the following 2D FK

equation(SP<sub>3</sub>)

$$\begin{cases} u_t - \Delta u + f(u) = g(x, y, t), & (x, y) \in \Omega, 0 < t \leq 1, \\ u(x, y, 0) = \sin(x) \sin(y), & (x, y) \in \Omega = [0, 1] \times [0, 1], \\ u(0, y, t) = u(2\pi, y, t) = 0, & y \in [0, 1], 0 < t \leq 1, \\ u(x, 0, t) = u(x, 2\pi, t) = 0, & x \in [0, 1], 0 < t \leq 1. \end{cases}$$

The exact solution of SP<sub>3</sub> is  $u(x, y, t) = e^{-t} \sin(x) \sin(y)$  and  $g(x, y, t) = (e^{-t} \sin(x) \sin(y))^3$ . Time increment  $\tau$  is fixed as 0.0001. This problem is a 2D problem, thus the OSM is needed for the computation. The implementation of OSM has been specifically modeled in Algorithm 1. The first step of it is that split it into four sub-problems by the Eq. (14)-(17). The second step is that each sub-problem can be solved by the CFDS6-OSM effectively. By making use of POD, the R-CFDS6-OSM is used to improve the efficiency of CFDS6-OSM. Table III gives the maximum error of CFDS6-OSM and computational time while Table IV gives the maximum error of R-CFDS6-OSM and computational time for different distributed points, which shows that the spatial errors of them are rapidly smaller and almost negligible and R-CFDS6-OSM saves a lot of computational time under same nodes. In addition, we fix  $\tau = 0.0001$  and  $h_x = h_y = h$ , then reduce  $h$  each time. It can be clearly seen that in Table III and Table IV the CFDS6-OSM and R-CFDS6-OSM are six-order accurate in space, since the maximum error for  $u$  is reduced by a factor about  $2^6$  each time. Moreover, the images in Figure 5-6 and Figure 7-8 are almost identical at  $t = 1$ . The difference in Figure 9 has confirmed that the R-CFDS6-OSM with fewer unknowns compared with CFDS6-OSM holds the significant information for solving the 2D FK equation.

TABLE III  
THE CONVERGENCE ORDER AND MAXIMUM ERROR OF CFDS6-OSM FOR SP<sub>3</sub> AT  $t = 1$

	Nodes	11 × 11	21 × 21	41 × 41
CFDS6-OSM	Max(error)	1.2756e-05	2.1649e-07	3.3664e-09
	Time(s)	0.527388	3.089644	88.453205
	Order	-	5.8807	6.0069

TABLE IV  
THE CONVERGENCE ORDER AND MAXIMUM ERROR OF R-CFDS6-OSM FOR SP<sub>3</sub> AT  $t = 1$

	Nodes	11 × 11	21 × 21	41 × 41
R-CFDS6-OSM	Max(error)	1.2756e-05	2.1649e-07	3.3675e-09
	Time(s)	0.392539	0.641083	1.553634
	Order	-	5.8807	6.0064

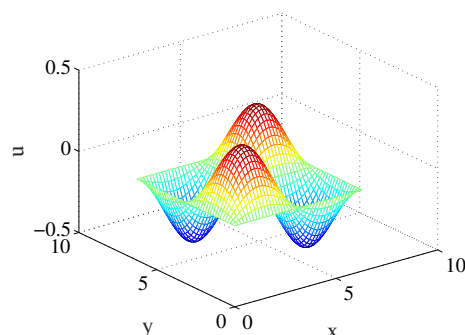


Fig. 5. The CFDS6-OSM( $N_x = N_y = 41$ ) solution at  $t = 1$  for SP<sub>3</sub>.

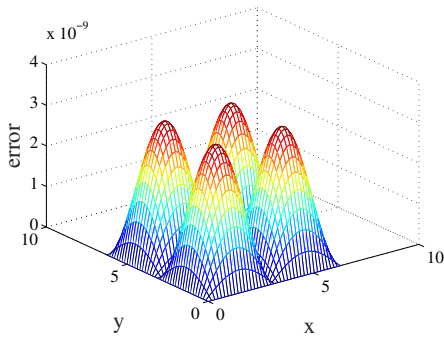


Fig. 6. The CFDS6-OSM( $N_x = N_y = 41$ ) error at  $t = 1$  for  $SP_3$ .

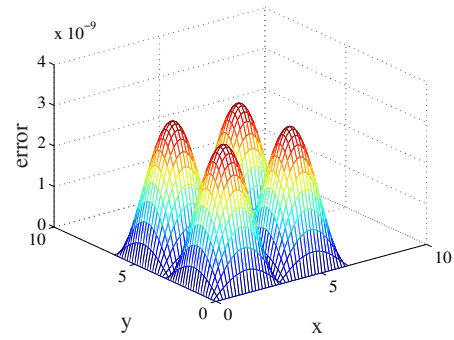


Fig. 8. The R-CFDS6-OSM( $N_x = N_y = 41$ ) error at  $t = 1$  for  $SP_3$ .

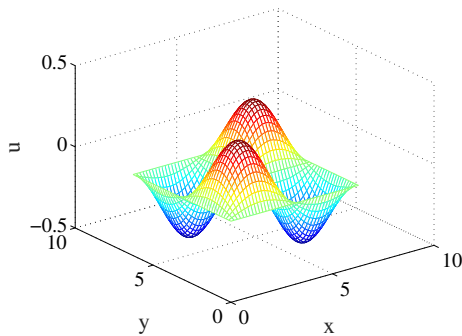


Fig. 7. The R-CFDS6-OSM( $N_x = N_y = 41$ ) solution at  $t = 1$  for  $SP_3$ .

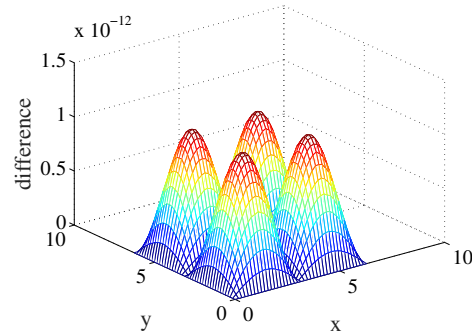


Fig. 9. The difference between R-CFDS6-OSM and CFDS6-OSM( $N_x = N_y = 41$ ) at  $t = 1$  for  $SP_3$ .

**Example 4:** We consider the following 2D EFK equation( $SP_4$ )

$$\begin{cases} u_t + \gamma \Delta^2 u - \Delta u + f(u) = 0, & (x, y) \in \Omega, 0 < t \leq 1, \\ u(x, y, 0) = \sin(x) \sin(y), & (x, y) \in \Omega = [0, 1] \times [0, 1], \\ u(0, y, t) = u(2\pi, y, t) = 0, & y \in [0, 1], 0 < t \leq 1, \\ u(x, 0, t) = u(x, 2\pi, t) = 0, & x \in [0, 1], 0 < t \leq 1. \end{cases}$$

Similar with Example 2, the numerical solution when  $N_x = N_y = 81$  in CFDS6 can be taken as the exact solution  $u$  approximately. We let  $\gamma = 1$  and  $\tau = 0.000001$ . This problem is much complicated than other examples, since it not only contains the mixed derivatives, but also has the fourth-order derivatives. The implementation of OSM has been analogously modeled in Algorithm 1. Firstly, we split it into four subproblems by the Eq. (14)-(17), then each subproblems can be solved, which indicates the effective of the OSM. The maximum absolute error in different nodes and the convergence of CFDS6-OSM and R-CFDS6-OSM are reported in Table V and Table VI respectively, where the expected six-order has been achieved. By comparing the computational time of R-CFDS6-OSM and CFDS6-OSM, it can be found the obvious advantages of the R-CFDS6-OSM. The numerical results are drawn in Figure 10-11 and Figure 12-13, which demonstrates that both of them have high accuracy with rapidly smaller and almost negligible. In additional, we also plot the difference between two schemes in Figure 14, which shows the R-CFDS6-OSM can maintain the important information.

TABLE V  
THE CONVERGENCE ORDER AND MAXIMUM ERROR OF CFDS6-OSM FOR  $SP_4$  AT  $t = 1$

	Nodes	11 × 11	21 × 21	41 × 41
CFDS6-OSM	Max(error)	5.3521e-07	9.0071e-09	1.3738e-10
	Time(s)	215.175615	1049.261344	4358.631622
	Order	-	5.8929	6.0348

TABLE VI  
THE CONVERGENCE ORDER AND MAXIMUM ERROR OF R-CFDS6-OSM FOR  $SP_4$  AT  $t = 1$

	Nodes	11 × 11	21 × 21	41 × 41
R-CFDS6-OSM	Max(error)	5.3521e-07	8.9989e-09	1.3953e-10
	Time(s)	92.714222	183.291991	343.417270
	Order	-	5.8942	6.0111

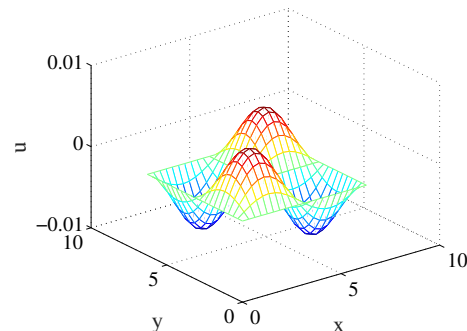


Fig. 10. The CFDS6-OSM( $N_x = N_y = 21$ ) solution at  $t = 1$  for  $SP_4$ .

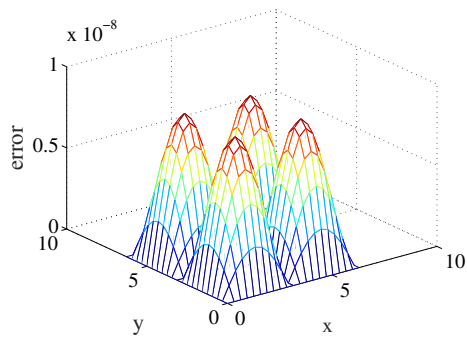


Fig. 11. The CFDS6-OSM( $N_x = N_y = 21$ ) error at  $t = 1$  for  $SP_4$ .

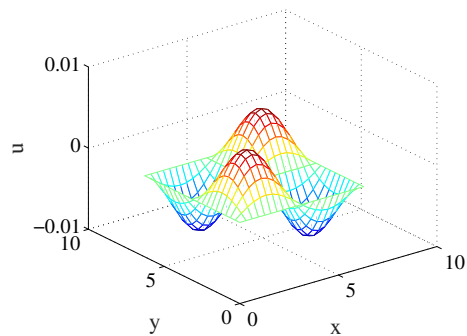


Fig. 12. The R-CFDS6-OSM( $N_x = N_y = 21$ ) solution at  $t = 1$  for  $SP_4$ .

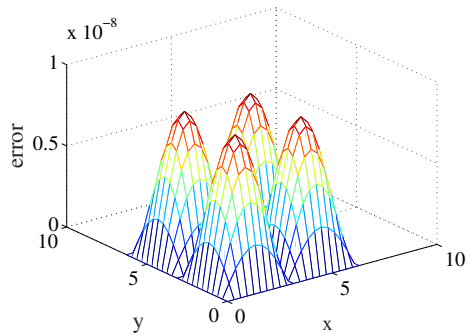


Fig. 13. The R-CFDS6-OSM( $N_x = N_y = 21$ ) error at  $t = 1$  for  $SP_4$ .

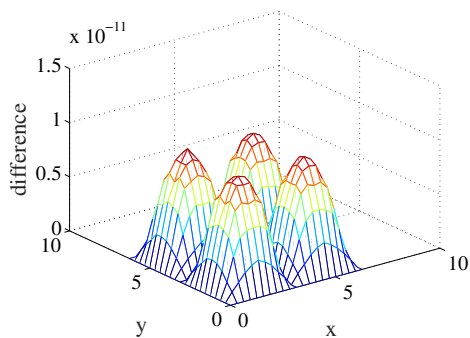


Fig. 14. The difference between R-CFDS6-OSM and CFDS6-OSM( $N_x = N_y = 21$ ) at  $t = 1$  for  $SP_4$ .

## VI. CONCLUSION

In this article, we have established the R-CFDS6-OSM for the numerical solution of two-dimensional EFK equation. We first decompose the two-dimensional EFK equation into a series of one-dimensional equation by the OSM, which is easy to be solved compared with the ADI. For the one-dimensional problems, the CFDS6 is used to solve it and the derivatives are approximated by the Eq. (2)-(5), then the RK4 method is used for solving the resulting system of ODEs. Lastly, the POD technique is employed to improve the computational efficiency of CFDS6 so that the R-CFDS6-OSM maintains all the superiority of CFDS6-OSM. The efficiency and reliability of our methods are demonstrated by the four numerical examples, which indicates the proposed method can appreciably improve the accuracy of numerical solution and save the time required for computation. In additional, OSM is an feasible way to deal with complicated problem containing mixed derivatives and the detailed algorithm is furnished. The implementation of R-CFDS6-OSM is very easy to program for the nonlinear equations. Therefore, the combination of R-CFDS6 based on POD and OSM can solve the two-dimensional EFK equation very successfully.

## ACKNOWLEDGMENT

The authors express their sincere thanks to the anonymous reviews for their valuable suggestions and corrections for improving the quality of this paper.

## REFERENCES

- [1] P. Coullet, C. Elphick, and D. Repaux, "Nature of spatial chaos," *Physical Review Letters*, vol. 58, no. 5, pp. 431–434, 1987.
- [2] G. Ahlers and D. S. Cannell, "Vortex-front propagation in rotating Couette-Taylor flow," *Physical Review Letters*, vol. 50, pp. 1583–1586, 1983.
- [3] P. Danumjaya and A. K. Pani, "Numerical methods for the Extended Fisher-Kolmogorov (EFK) equation," *International Journal of Numerical Analysis and Modeling*, vol. 3, no. 2, pp.186–210, 2006.
- [4] T. Kadri and K. Omrani, "A second-order accurate difference scheme for an extended Fisher-Kolmogorov equation," *Computers & Mathematics with Applications*, vol. 61, no. 2, pp. 451–459, 2011.
- [5] N. Khiari and K. Omrani, "Finite difference discretization of the extended Fisher-Kolmogorov equation in two dimensions," *Computers & Mathematics with Applications*, vol. 62, no. 11, pp. 4151–4160, 2011.
- [6] T. Gudi and H. S. Gupta, "A fully discrete  $C^0$  interior penalty Galerkin approximation of the extended Fisher-Kolmogorov equation," *Journal of Computational and Applied Mathematics*, vol. 247, no. 1, pp. 1–16, 2013.
- [7] P. Danumjaya and A. K. Pani, "Orthogonal cubic spline collocation method for the extended Fisher-Kolmogorov equation," *Journal of Computational and Applied Mathematics*, vol. 174, no. 1, pp. 101–117, 2005.
- [8] X. D. Ye, "The fourier collocation method for the Cahn-Hilliard equation," *Computers & Mathematics with Applications*, vol. 44, no. 1, pp. 213–229, 2002.
- [9] J. C. Li, "High-order finite difference schemes for differential equations containing higher derivatives," *Applied Mathematics and Computation*, vol. 171, no. 2, pp. 1157–1176, 2005.
- [10] J. C. Li and Y. T. Chen, "Computational Partial Differential Equations Using MATLAB," CRC Press, New York, 2009.
- [11] B. Düring and A. Pitkin, "High-order compact finite difference scheme for option pricing in stochastic volatility jump models," *Journal of Computational and Applied Mathematics*, vol. 355, pp. 201–217, 2019.
- [12] J. C. Li, Y. T. Chen, and G. Q. Liu, "High-order compact ADI methods for parabolic equations," *Computers & Mathematics with Applications*, vol. 52, no. 8, pp. 1343–1356, 2006.
- [13] J. C. Li and M. R. Visbal, "High-order compact schemes for nonlinear dispersive waves," *Journal of Scientific Computing*, vol. 26, no. 1, pp. 1–23, 2006.
- [14] Q. H. Feng, "Compact difference schemes for a class of space-time fractional differential equations," *Engineering Letters*, vol. 27, no. 2, pp. 17–25, 2019.

- [15] D. W. Deng and J. Q. Xie, "High-order exponential time differencing methods for solving one-dimensional burgers' equation," *IAENG International Journal of Computer Science*, vol. 43, no. 2, pp. 167–175, 2016.
- [16] D. Ghosh and E. M. Constantinescu, "Nonlinear compact finite-difference schemes with semi-implicit time stepping," *Lecture Notes in Computational Science and Engineering*, vol. 106, pp. 237–245, 2015.
- [17] H. W. Sun and L. Z. Li, "A CCD-ADI method for unsteady convection-diffusion equations," *Computer Physics Communications*, vol. 185, no. 3, pp. 790–797, 2014.
- [18] S. Y. Zhai, X. L. Feng, and Y. N. He, "A new method to deduce high-order compact difference schemes for two-dimensional Poisson equation," *Applied Mathematics and Computation*, vol. 230, pp. 9–26, 2014.
- [19] A. Mohebbi and M. Dehghan, "High-order compact solution of the one-dimensional heat and advection-diffusion equations," *Applied Mathematical Modelling*, vol. 34, no. 10, pp. 3071–3084, 2010.
- [20] A. Mohebbi, M. Abbaszadeh, and M. Dehghan, "Compact finite difference scheme and RBF meshless approach for solving 2D Rayleigh-Stokes problem for a heated generalized second grade fluid with fractional derivatives," *Computer Methods in Applied Mechanics and Engineering*, vol. 264, pp. 163–177, 2013.
- [21] Z. D. Luo, H. Li, Y. J. Zhou, and X. M. Huang, "A reduced FVE formulation based on POD method and error analysis for two-dimensional viscoelastic problem," *Journal of Mathematical Analysis and Applications*, vol. 385, no. 1, pp. 310–321, 2012.
- [22] Z. D. Luo, Y. J. Zhou, and X. Z. Yang, "A reduced finite element formulation based on proper orthogonal decomposition for Burgers equation," *Applied Numerical Mathematics*, vol. 59, no. 8, pp. 1933–1946, 2009.
- [23] M. Dehghan and M. Abbaszadeh, "A combination of proper orthogonal decomposition-discrete empirical interpolation method (POD-DEIM) and meshless local RBF-DQ approach for prevention of groundwater contamination," *Computers & Mathematics with Applications*, vol. 75, no. 4, pp. 1390–1412, 2018.
- [24] Z. D. Luo and F. Teng, "A reduced-order extrapolated finite difference iterative scheme based on POD method for 2D Sobolev equation," *Applied Mathematics and Computation*, vol. 329, pp. 374–383, 2018.
- [25] M. Seydaoğlu, "An accurate approximation algorithm for Burgers' equation in the presence of small viscosity," *Journal of Computational and Applied Mathematics*, vol. 344, pp. 473–481, 2018.
- [26] P. C. Jain and D. N. Holla, "Numerical solutions of coupled Burgers' equation," *International Journal of Non-Linear Mechanics*, vol. 13, no. 4, pp. 213–222, 1978.
- [27] P. C. Jain, R. Shankar, and T. V. Singh, "Cubic spline technique for solution of Burgers' equation with a semi-linear boundary condition," *Communications in Applied Numerical Methods banner*, vol. 8, no. 4, pp. 235–242, 1992.
- [28] H. H. Gidey and B. D. Reddy, "Operator-splitting methods for the 2D convective Cahn-Hilliard equation," *Computers & Mathematics with Applications*, vol. 77, no. 12, pp. 3128–3153, 2019.
- [29] J. Sun and J. A. Eichholz, "Splitting methods for differential approximations of the radiative transfer equation," *Applied Mathematics and Computation*, vol. 322, pp. 140–150, 2018.
- [30] S. K. Lele, "Compact finite difference schemes with spectral-like resolution," *Journal of Computational Physics*, vol. 103, no. 1, pp. 16–42, 1992.
- [31] J. D. Lambert, "Numerical Methods for Ordinary Differential Systems: The Initial Value Problem," John Wiley & Sons, New York, 1991.
- [32] D. W. Peaceman and H. H. Rachford, Jr, "The numerical solution of Parabolic and Elliptic differential equations," *Journal of the Society for Industrial and Applied Mathematics*, vol. 3, no. 1, pp. 28–41, 1955.
- [33] M. Seydaoğlu, U. Erdoğan, and T. Öziş, "Numerical solution of burgers' equation with high order splitting methods," *Journal of Computational and Applied Mathematics*, vol. 291, no. 1, pp. 410–421, 2016.
- [34] H. Holden, C. Lubich, and N. H. Risebro, "Operator splitting for partial differential equations with Burgers nonlinearity," *Mathematics Of computation*, vol. 82, pp. 173–185, 2013.
- [35] R. Dutta, H. Holden, U. Koley, and N. H. Risebro, "Operator splitting for the Benjamin-Ono equation," *Journal of Differential Equations*, vol. 259, no. 11, pp. 6694–6717, 2015.
- [36] N. Gücüyenen and G. Tanoğlu, "On the numerical solution of Korteweg-de Vries equation by the iterative splitting method," *Applied Mathematics and Computation*, vol. 218, no. 3, pp. 777–782, 2011.
- [37] Z. D. Luo and G. Chen, "Proper orthogonal decomposition methods for partial differential equations," Elsevier Press, Amsterdam, 2018.